

SEND: A Situation-Aware Emergency Navigation Algorithm with Sensor Networks

Chen Wang, *Member, IEEE*, Hongzhi Lin, Rui Zhang, and Hongbo Jiang, *Senior Member, IEEE*

Abstract—When emergencies happen, navigation services that guide people to exits while keeping them away from emergencies are critical in saving lives. To achieve timely emergency navigation, early and automatic detection of potential dangers, and quick response with safe paths to exits are the core requirements, both of which rely on continuous environment monitoring and reliable data transmission. Wireless sensor networks (WSNs) are a natural choice of the infrastructure to support emergency navigation services, given their relatively easy deployment and affordable costs, and the ability of ubiquitous sensing and communication. Although many efforts have been made to WSN-assisted emergency navigation, almost all existing works neglect to consider the hazard levels of emergencies and the evacuation capabilities of exits. Without considering such aspects, existing navigation approaches may fail to keep people farther away from emergencies of high hazard levels and would probably encounter congestions at exits with lower evacuation capabilities. In this paper, we propose SEND, a situation-aware emergency navigation algorithm, which takes the hazard levels of emergencies and the evacuation capabilities of exits into account and provides the mobile users the safest navigation paths accordingly. We formally model the situation-aware emergency navigation problem and establish a hazard potential field in the network, which is theoretically free of local minima. By guiding users following the descend gradient of the hazard potential field, SEND can thereby achieve guaranteed success of navigation and provide optimal safety. The effectiveness of SEND is validated by both experiments and extensive simulations in 2D and 3D scenarios.

Index Terms—Emergency navigation, situation-aware, sensor networks, exit capability, hazard potential field

1 INTRODUCTION

BENEFITING from recent advances in wireless sensor network (WSN) technologies, large-scale deployment of WSNs has become viable and affordable [1], [2], [3], [4], which ever used to serve as an increasingly popular platform to engage continuous environment monitoring [5], [6], [7], [8]. Recently there is a trend to incorporate WSNs into emergency navigation systems [9], [10], [11], [12], aiming at providing early and automatic detection of potential dangers, such as geologic disasters, wildfire hazards and oil/gas leakages, and navigating people to safe exits while keeping them away from emergencies.

This work considers such a WSN-assisted emergency navigation problem by utilizing the sensor network infrastructure as a cyber-physical system. In this mobile scenario, people are equipped with communicating devices like mobile phones that can talk to the sensors. When emergencies happen and mobile users are trapped in the field, the sensor network explores the emergencies and provides necessary guidance information to the mobile users, so that the users can be eventually guided to safe exits through ubiquitous interactions with sensors.

Although many WSN-assisted emergency navigation methods have been proposed [9], [10], [11], [12], [13], [14], [15], almost all existing approaches equally regard the hazard levels of different emergencies, as shown in Fig. 1a. As elaborated in [16], [17], different emergencies could occur concurrently with each corresponding to a specific hazard level. Considering a field with poisonous gas leakage, the hazard levels of emergencies are closely related to the poisonousness of the leaked gas. For instance, chlorine gas is much more fatal than carbon monoxide [18]. Furthermore, different sizes of leakage holes lead to different amounts of gas leakage per unit time. Therefore, when planning emergency navigation paths, people should be kept farther away from chlorine compared with carbon monoxide. A similar idea has been elaborated in the field of chemical process safety [19]. The navigation approaches without considering different hazard levels of emergencies may fail to provide necessary protection in the navigation process.

Another limitation of existing works is that the evacuation capabilities of exits are generally assumed to be equal. When there are more than one safe exit, which is very common in reality, existing methods [9], [12], [13], [14] simply guide people to the nearest one for the sake of timeliness, as shown in Fig. 1c. Such strategy would probably guide a majority of people to the same exit, which potentially causes extreme congestions at the exit and significantly prolongs the emergency navigation time while leaving other exits of low usages. This can be confirmed according to an investigation report in 2015 from ACT Emergency Services Agency [20], that over 46 percent of victims in high-rise apartment fire crash in Europe are killed in the congestions near the exits, which keep off their last hope

• C. Wang, H. Lin, and H. Jiang are with the School of Electronic Information and Communications, Huazhong University of Science and Technology, Wuhan, Hubei 430074, P.R. China.

E-mail: {cwangwu, eihongzhilin2012, hongbojiang2004}@gmail.com.

• R. Zhang is with the School of Computer Science and Technology, Wuhan University of Technology, Wuhan, Hubei 430070, P.R. China.
E-mail: zhangrui@whut.edu.cn.

Manuscript received 6 Dec. 2015; revised 15 Apr. 2016; accepted 26 May 2016. Date of publication 7 July 2016; date of current version 2 Mar. 2017.

For information on obtaining reprints of this article, please send e-mail to: reprints@ieee.org, and reference the Digital Object Identifier below.

Digital Object Identifier no. 10.1109/TMC.2016.2582172

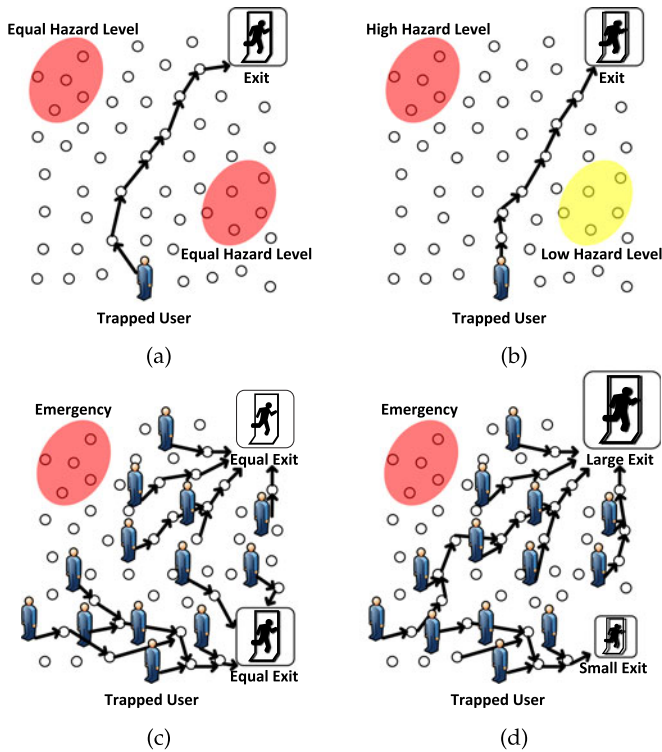


Fig. 1. Illustration of situation-aware emergency navigation with a 2D WSN. The emergency navigation paths when (a) there are equal hazard levels of emergencies, (b) the hazard level is higher at the red marked area and lower at the yellow marked area, (c) the two exits have equal evacuation capabilities, and (d) one exit has higher evacuation capability than the other.

for survival. Hence, it is rather necessary to take the evacuation capabilities of exits into consideration during the emergency navigation.

Therefore, we can arrive at the plain fact that a practical and efficient emergency navigation scheme should be *situation-aware*, which means that we should take into consideration both the hazard levels of concurrent emergencies, as shown in Fig. 1b, and the evacuation capabilities of exits, as shown in Fig. 1d.

Despite its importance, on the down side, we capitalize that it is not straightforward to design such a situation-aware emergency navigation. It is non-trivial to directly extending existing methods [9], [10], [15] which inherently aim at navigating users along the paths with equal distances to emergencies. The main challenge here is how to define the safety properly, incorporating the impacts of both different hazard levels of emergencies and different capabilities of the exits at the same time.

Let us take the road map based navigation approach [10], [15] (RMN for short) for instance. RMN first builds the road map by connecting the medial axis (a path with equal distance to the hazards) of the network, with a tail route connecting the exits, and then guides users along the road map with preset directions on the road segments. To incorporate the impact of different hazard levels of emergencies, the medial axis may be built as the weighted medial axis (e.g., by assigning different weights to the distances to different hazards to reflect different hazard levels). However, it is still difficult to incorporate the impact of different capabilities of the exits at the same time. For one thing, the evacuation capability

of an exit represents the safety level instead of the hazard level, but a unified treatment is far from ready-made. For another, it is not easy to extend the way of direction identification on the backbone, such that the direction can divert the flows to exits in accordance with their capabilities.

To address the above issues, in this paper, we present SEND, a situation-aware emergency navigation algorithm, which takes the hazard levels of emergencies and the evacuation capabilities of exits into account and provides the mobile users the safest navigation paths accordingly. Motivated by the fact that the natural gradients of some physical quantities always follows a natural diffusion law, e.g., water always flows from the place with a higher gravity potential to that with a lower gravity potential, we thus propose to model the hazard levels of emergencies and the evacuation capabilities of exits as hazard potentials with positive and negative values, respectively. Then we establish a hazard potential field in the network, which is theoretically free of local minima. By guiding users following the descend gradient of the hazard potential field, our method can thereby achieve guaranteed success of navigation and provide optimal safety to users. Fig. 2 shows an example of the resulted potential fields and navigation paths by SEND in scenarios of Fig. 1.

To the best of our knowledge, SEND is the first situation-aware emergency navigation scheme, considering the impacts of both the hazard levels of emergencies and the evacuation capabilities of exits. It is fully distributed and does not require any location information. It is more robust to emergency dynamics since the constructed hazard potential field reflects more global properties of the underlying connectivity. Both small-scale testbed experiments and extensive simulations on large-scale WSNs, in both 2D and 3D scenarios, validate the effectiveness and efficiency of SEND.

The remainder of this paper is organized as follows. We present the theoretical foundation in Section 2 and elaborate on our approach in Section 3, with further discussions in Section 4. We implement SEND on a small-scale testbed in Section 5, and present the experiment results in Section 6. Extensive simulations with large-scale networks are conducted in Section 7, and the related works are presented in Section 8. Finally Section 9 concludes this paper.

2 THEORETICAL FOUNDATION

In this section, we propose a unified model to quantify the safety in both 2D and 3D continuous domains. To clarify, we may use hazard instead of safety to describe emergencies, which is more intuitive to depict emergencies than safety, and is the opposite aspect of safety. We first define *single point hazard* to quantify the hazard of an arbitrary location in the considered area. Then, we investigate the *mean value property* of the *hazard potential field*, which is derived from the single point hazard. Note that the mean value property is the theoretical foundation to transfer safety definition to discrete domain (WSNs), as will be discussed in Section 3. At last, we formally define the objective of our emergency navigation algorithm.

2.1 Network Model

We consider a field where there may be different emergency events and multiple exits with different evacuation

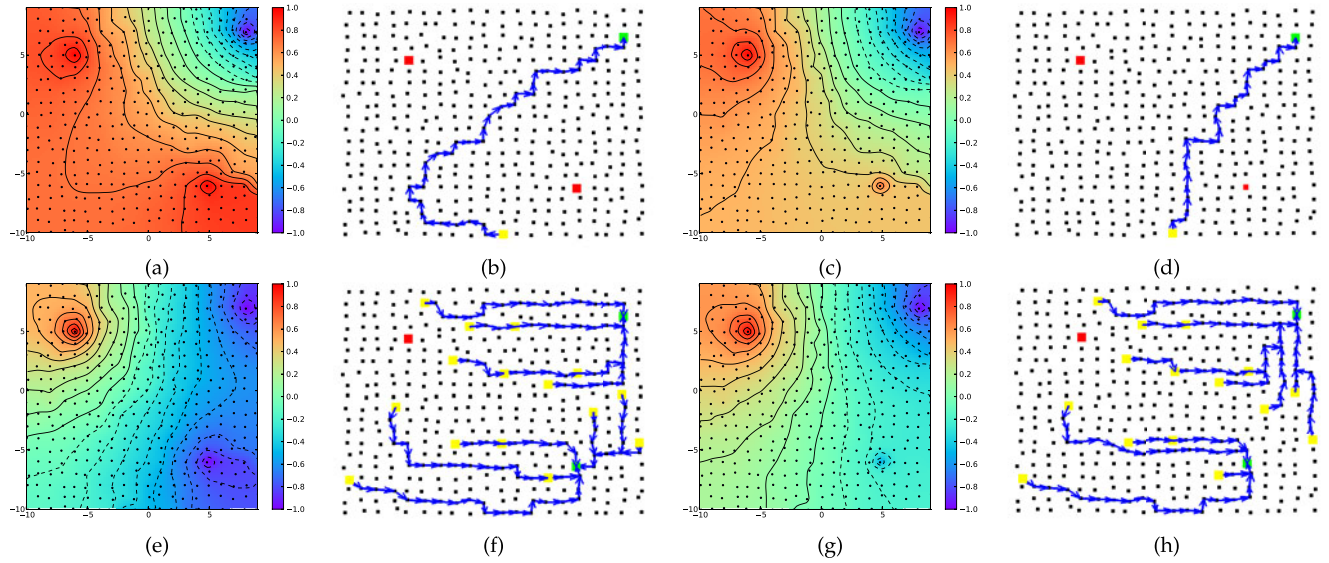


Fig. 2. Illustration of the hazard potential fields and the navigation paths in scenarios of Fig. 1. The solid red rectangles are emergency nodes; the solid green rectangles are exit nodes; nodes marked in yellow represent trapped users. The hazard potential field and navigation path computed by SEND when (a), (b) the emergencies have equal hazard levels, (c), (d) the emergencies have unequal hazard levels (the top-left emergency has a higher hazard potential), (e), (f) the exits has equal capabilities, and (g), (h) the exits has unequal capabilities (the upper exit has a larger evacuation capability).

capabilities. People inside the field are anticipated to be immediately navigated to appropriate exits while being far away from emergencies in proportion to corresponding hazard levels. Specifically, the emergency navigation paths are expected to be farther away from areas with higher hazard levels, and more people should be guided to exits with higher evacuation capabilities. On the basis of these observations, we thus formulate the navigation problem as a path planning problem.

Let \mathcal{R} denote a 2D or 3D continuous open space, which represents the field of interest. Inside \mathcal{R} , there exist n safe exits, which are located at points $P_e = \{p_e^i \mid i = 1, 2, \dots, n\}$. Each exit is assigned a weight based on its evacuation capability. Suppose that in \mathcal{R} , there are m emergencies occurring at points $P_d = \{p_d^j \mid j = 1, 2, \dots, m\}$. Each emergency is also assigned with a weight based on its hazard level. We denote the set of weights of exits and emergencies by $W_e = \{w_e^i \mid i = 1, 2, \dots, n\}$ and $W_d = \{w_d^j \mid j = 1, 2, \dots, m\}$, respectively. Table 1 summarizes the notations used in our model.

TABLE 1
Notation Summary

Symbol	Definition
\mathcal{R}	a continuous open space in 2D or 3D
P_d	the set of points where emergencies occur
P_e	the set of points where safe exits locate
$ pq $	the euclidean distance between points p and q
\vec{pq}	the vector connecting the points p and q
W_d	the set of weights of safe exits
W_e	the set of weights of emergencies
$G(V, E)$	a sensor network as an undirected graph
V	the set of sensor nodes
E	the set of the links between neighbor sensors
V_d	the set of sensors with hazardous readings
V_e	the set of sensors located at exits
V_n	the set of sensors with normal readings
$F(v)$	the hazard potential function of sensor node v

2.2 Single Point Hazard

An emergency navigation problem is essentially to find the optimal emergency navigation paths in terms of safety. Quantifying the safety of a path is equal to quantifying the hazard of a path, which is closely related to emergency. In the following, we first focus on the hazard of an arbitrary point in the field of interest, which is the basis of finding the safest navigation path.

Hazard Intensity. To quantify the hazard of a location, we introduce a novel metric called *hazard intensity*, which is based on the observation that for an internal user, one may feel more hazardous threat when getting closer to emergencies, and would feel safer when getting closer to exits. Furthermore, the feeling should be a vector that has the ability to describe the direction of the hazardous event. Fig. 3 shows an illustration of this simple observation.

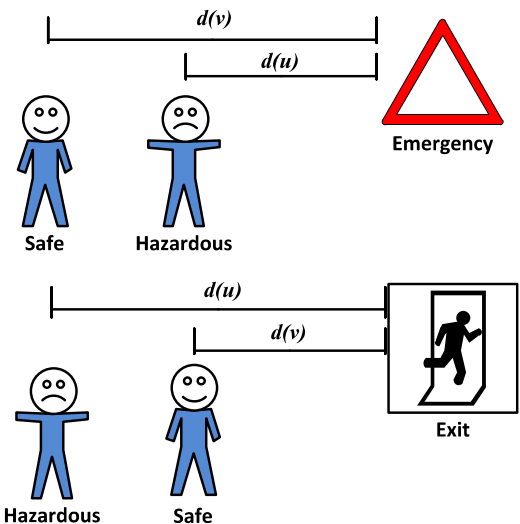


Fig. 3. Our observation: the user feels safer if he/she is farther away from the danger and closer to the exit.

It is noticed that this observation has been validated by U.S. Geological Survey EROS Data Center and U.S. Forest Service, both of which take *Fire Potential Index* (FPI) as a way to evaluate the forest fire hazard feeling [21]. It is indicated that, the emergencies with higher hazard levels have higher probability to jeopardize the users and the exits with higher evacuation capabilities yield higher probability for users to get evacuated.

Inspired by the observation, we remark that any function can be used to represent the hazardous threats, as long as it is reversely proportional to the Euclidean distance between the emergencies. Accordingly, we define a metric, *hazard intensity* $\vec{I}(p)$, which quantifies the hazardous threat at point p as follows:

$$\vec{I}(p) = \sum_{j=1}^m w_j \frac{\vec{pp}_d^j}{|pp_d^j|^3} - \sum_{i=1}^n w_i \frac{\vec{pp}_e^i}{|pp_e^i|^3}. \quad (1)$$

Obviously, the hazard intensity satisfies superposition principle. In other words, the hazard intensity at point p induced by multiple emergencies and exits is the sum of the responses that would have been caused by each stimuli separately.

Hazard Potential. The hazard intensity reflects only an instant feeling of the user, which is not enough to quantify the hazard of a single point. To this end, we introduce a function called *hazardous potential* $\Phi(p)$, which represents the total hazardous intensity one user has starting from infinity and ending at point p . We choose infinity as a common reference point to evaluate the hazard potential in different spaces. Therefore, we define the hazard potential $\Phi(p)$ of point p as follows:

$$\Phi(p) = \int_{\infty}^p \vec{I}(l) dl. \quad (2)$$

The hazard potential describes the cumulative hazard intensity that the user should take when moving from p to infinity. Accordingly, the difference of hazard potential $\Phi(p) - \Phi(q)$ between points p and q can well measure which point is more dangerous to the user. Specifically, a positive value of the difference of hazard potential indicates a higher chance of the user at p to be harmed than at q . Therefore, the hazard potential can be used as a tool to quantitatively measure the amount of hazard of a single point.

2.3 Hazard Potential Field

Armed with the definition of single point hazard, we are now able to define the hazard potential field in a continuous space, which plays an essential role in finding the safest paths for trapped users.

Based on Eqs. (1) and (2), a hazard potential field Φ in a continuous space \mathcal{R} satisfies

$$\nabla\Phi(p) = I(p). \quad (3)$$

According to *Gauss's Law*, the potential field Φ satisfies *Laplace's equation* [22]:

$$\nabla I(p) = \nabla^2\Phi = 0. \quad (4)$$

Note that the function satisfying Laplace's equation is called *harmonic function* and has the *mean value property*.

Mean Value Property. If $B(p, r)$ is a ball with the center at point p and the radius of r in the open space \mathcal{R} , then the value of $\Phi(p)$ at the center of the ball is given by the average value of Φ on the surface of the ball. In addition, $\Phi(p)$ is also equal to the average value of Φ in the interior of the ball. Accordingly, we have

$$\Phi(p) = \frac{1}{|B(p, r)|} \int_{B(p, r)} \Phi d\delta, \quad (5)$$

where $|B(p, r)|$ is the volume of the ball in \mathcal{R} and δ is the surface measure.

The mean value property implies that the hazard potential of a point in \mathcal{R} can be easily calculated with information of the points within a disk of an arbitrary radius r . This property naturally fits the well-known unit disk graph (UDG) communication model [23] in WSNs. Thus we can take advantage of the mean value property of the hazard potential field to solve the proposed safest path planning problem in a fully *distributed* manner, by utilizing only the information of node's one hop neighbors.

2.4 Path Hazard Metric and the Safest Path

We are interested in finding the safest path from an arbitrary point $p \in P_n$ to an appropriate exit $p_e^j \in P_e$. The primary challenge of such problem is to choose the safest path among huge amounts of paths, which start from p and end at p_e^j . So in the first step, we have to design a *path hazard metric* to quantify the hazard of a path. As we discussed before, the location of point p is more harmful to the user than that of point q if $\Phi(p) > \Phi(q)$. Intuitively, the hazard of a path can be quantitatively measured as the maximum hazard potential of the points on the path. Therefore, we can define the hazard of a path C as

$$D(C) = \max\{\Phi(p) | p \in C\}. \quad (6)$$

Our objective is to find the safest path C^* from point p to point p_e^j , such that the maximum hazard along the path is minimum, i.e.,

$$C^* = \arg \min_C D(C). \quad (7)$$

Although we have this guideline to select the safest path among all possible paths, we still face several problems to implement it in discrete WSNs where many constraints are needed to be considered. We will discuss this in the next section.

3 SEND ALGORITHM

Based on the aforementioned theoretical foundation in continuous domains, in this section, we further describe the details of SEND algorithm in discrete sensor networks. We first define hazard potential field in the network, which is the discrete counterpart of hazard potential field in continuous domains. Then we propose an iterative method to establish the hazard potential field by sensor readings in a fully distributed manner. Based on the established hazard potential field, we next propose a path selection method and theoretically prove that the selected paths guarantee successful navigation and are optimal in terms of safety. We

also propose a scheme to accelerate the establishment of the hazard potential field, in order to achieve timely emergency navigation.

3.1 Hazard Potential Field in Sensor Networks

A relatively dense sensor network can be viewed as a discrete approximation of a continuous space \mathcal{R} . The sensor network is then modelled as an undirected graph $G(V, E)$, where V is the set of vertices that represent the sensor nodes, and E denotes the set of edges that represent the communication links between sensor nodes. Let V_d denote the sensors with hazardous readings, V_e the sensors at the exits, and V_n the remaining sensors with normal readings.

We first define the hazard potential field in discrete WSNs. According to the mean value property of the hazard potential field in Section 2, the hazard potential function $F(v)$ of a sensor node v satisfies the following equation:

$$F(v) = \frac{1}{|N(v)|} \sum_{u \in N(v)} F(u), \quad v \in V_n, \quad (8)$$

where $N(v)$ is the set of neighbor nodes of node v and $|N(v)|$ is the cardinality of $N(v)$.

However, when emergencies occur across the sensor field, only the sensor nodes near the emergencies and exits have abnormal readings. It is not easy for the hazard potential functions of all sensors to satisfy Eq. (8). Therefore, we need to distribute these readings to the whole network and establish the hazard potential field.

3.2 Iterative Hazard Potential Field Establishment

Based on the mean value property, we propose an iterative method to distribute abnormal readings to the network and establish the hazard potential field in a fully distributed manner. To be more concrete, when there is no emergency, each node $v \in V_n$ is assigned a hazard potential value as 0, while each sensor $v \in V_e$ is assigned a negative hazard potential value reversely proportional to its capability. When the emergency happens, each sensor $v \in V_d$ will set its hazard potential value with a positive value proportional to the hazard level of its reading.

Theoretically, the hazard potential of the sensor $v \in V_d$ could be any positive number, and a larger potential represents a larger hazardous reading; likewise, the potential of the sensor $v \in V_e$ could be any negative number, and a larger potential represents a smaller capability. In our implementation, the potential of the sensor with a hazardous reading is set in $[0, 1]$, while the potential of the exit is set in $[-1, 0]$. For example, in the experiment in Section 6, we set the potential of the sensor with a small (resp. large) hazardous reading with 0.5 (resp. 1), and the potential of the small (resp. large) exit with -0.5 (resp. -1).

At first, every sensor $v \in V_n \cup V_e$ has set its hazard potential value. When the emergency happens, every sensor $v \in V_d$ begins to set its hazard potential value. At this time, the potentials of the sensors with hazardous readings, the exits and other sensors with normal readings are positive, negative and zero, respectively. When the hazard potential

function $F(v)$ of $v \in V_d \cup V_e$ is fixed, every sensor $v \in V_n$ conducts the iteration as follows:

$$F^{(k+1)}(v) \leftarrow \frac{1}{|N(v)|} \sum_{u \in N(v)} F^k(u), \quad v \in V_n. \quad (9)$$

According to *Dirichlet boundary condition* [22], this iterative process will finally converge if the hazard potential $F(v)$ at the position of $v \in V_d \cup V_e$ is set to be constant. Once the hazard potentials of all nodes in the network are stable, the final $F(v)$ is the hazard potential of node $v \in V$, and it satisfies Eq. (8).

3.3 Safest Paths Identification

With the established hazard potential field in the sensor network, it is straightforward to select the safest paths among all possible paths that link the internal users and safe exits. In particular, every user initiates the path selection by communicating to a nearby sensor node $v \in V_n$ with a normal reading, which then selects a neighbor node $u \in N(v)$ with the smallest hazardous potential $F(u)$ among its neighbors and sets it as the next destination node. By repeating this process, the emergency navigation path comes into being and is guaranteed to reach the sensor at the location of one exit. This process can then be expressed as

$$S(v) = \arg \min_{u \in N(v)} F(u), \quad (10)$$

where $S(v)$ denotes the next destination node of the current sensor v .

There are two salient properties for the paths selected in this manner as follows.

Theorem 1. *The emergency navigation paths selected by the proposed method guarantee successful navigation.*

Proof. Given the established hazard potential field in the sensor network, the hazard potential $F(v)$ of any node $v \in V_n$ satisfies Eq. (8), which means the hazard potential $F(v)$ is the mean value of the hazard potential among the neighbors of v . Note that according to the min-max principle [24], in our case where there are several fixed positive hazard potentials (of nodes in V_d) and negative hazard potentials (of nodes in V_e), there is no plateau region where all the neighbors have the same hazard potentials with v . Therefore, the hazard potential field is guaranteed to be free of local minima except for the hazard potentials of nodes in V_e . As a result, all the generated paths starting from any node $v \in V_n$ in the field will only end at the exit nodes $v_j \in V_e$ which are the global minima. Thus, Theorem 1 holds. \square

Theorem 1 shows that the selected paths provide users guaranteed successful navigation. Each user in the field will never be trapped when emergencies happen. Only the guaranteed successful navigation is not sufficient for the safety of users. Therefore we next show by the following theorem that the selected paths also provide optimal safety.

Theorem 2. *The navigation paths selected by the proposed method are optimal in terms of safety.*

Proof. In Section 2, we elaborate on the quantification problem of the safety of a path. The safety of a path is the

opposite aspect of the hazard of a path. If we can prove that the paths selected by the proposed method provide the least hazard, then the paths are optimal in terms of safety. Considering a path C that starts from point p and ends at exit point $v_j \in V_e$, the maximal hazard potential on C is at the initial point p according to Eq. (8). In line with the path selection method, the selected paths always go along the direction of the gradient of the hazard potential field. As a result, the point with the maximum hazard potential on the path C is the starting point p . In other words, the path hazard metric $D(C)$ equals $F(p)$ at the initial node p of the selected path. Accordingly, there are no paths having the same starting and ending points while at the same time with smaller $D(C)$ than the selected paths. Therefore the navigation paths selected by the proposed method provide the least hazard and thus are optimal in terms of safety. \square

Theorem 2 guarantees the safety of the paths selected by the proposed method. The above two theorems together prove that the emergency navigation paths selected by our method are the safest for the emergency navigation of the trapped users. Fig. 2 shows the established hazard potential field as well as the generated safest paths of our algorithm in different scenarios.

3.4 Accelerated Hazard Potential Field Establishment

As emergency navigation is a time critical application, we need to pay special attention to the time consumed on path planning. Centralized methods such as *Gauss Seidel method* [25] are able to speed up the convergence; however, they can not work in a distributed manner and require a relatively long time to collect all the sensor data to a sink. Based on the local information of each sensor node, we consider to utilize the *multi-step forward prediction* technique to boost the hazard potential field establishing process.

The key idea of the accelerated method is to estimate the multi-step forward iterative value of each sensor based on a small amount of preceding iterative hazard potential function values. By extrapolation, we can then predict the multi-step forward hazard potential function value of each sensor. As a result, the iteration process can skip over a number of iterations, with the help of the estimated value, and jump directly to multiple steps forward. By doing so, we can significantly reduce the number of iterations and thus boost up the convergence speed of the hazard potential field establishing process.

To this end, we propose to utilize *cubic extrapolation* [26]. The reason why we choose cubic extrapolation is threefold. First, we aim to design a localized protocol with the capability to be implemented in large scale sensor networks. Cubic extrapolation fits our requirements by using only local and incomplete information to reduce the redundancy of the iteration. Second, the memory of each sensor in the network is limited due to the hardware constraints of the sensors. Cubic extrapolation uses only a constant number of the past time series to estimate multi-step forward values of the hazard potential. Last but not least, considering the dynamics of sensing environment, cubic extrapolation is an input-adaptive method, which is robust in dynamic environments.

Cubic extrapolation works as follows. In the hazard potential field establishing phase, each sensor node v memorizes a time series $F^1(v), F^2(v), \dots, F^k(v)$. Let time k be the independent variable and $F^k(v)$ be the dependent variable representing the hazard potential value in the k th round of iteration. We assume that the iterative value $F^k(v)$ can be expressed as a point on the third-order curves that traverse at least four preceding iterative values $F^{k-i}(v)$, $i = 1, 2, 3, 4$. This assumption allows us to estimate a k -step forward value of $F(v)$ using at least four known values. The formulation of the process thus can be expressed as follows:

$$F^{k-i}(v) = \lambda_1(k-i)^3 + \lambda_2(k-i)^2 + \lambda_3(k-i) + \lambda_4, \quad (11)$$

where $i = 1, 2, 3, 4$, indicating that we have four unknown variables along with four equations. Thus we can figure out $\lambda_1, \lambda_2, \lambda_3, \lambda_4$ without much effort, and then use them to solve the following equation:

$$F^k(v) = \lambda_1(k)^3 + \lambda_2(k)^2 + \lambda_3(k) + \lambda_4, \quad (12)$$

Accordingly, we can estimate multi-step forward iterative results of $F(v)$ using only four preceding values. For instance, when the iteration in Eq. (8) produces a time series $\{F^1(v), F^2(v), F^3(v), F^4(v)\}$, we can get the unknown variables of $\{\lambda_1, \lambda_2, \lambda_3, \lambda_4\}$. Hence, in accordance with Eq. (12), we can easily estimate the $(k+4)$ -step forward iterative value $F^{k+4}(v)$ of the node v , where k represents the *step length* of our extrapolation. By skipping k -step iteration, the redundancy of the iterative process of Eq. (8) is significantly reduced and thus the hazard potential field establishment of the whole network can be notably accelerated.

4 DISCUSSIONS

4.1 Reacting to Emergency Dynamics

Due to emergency dynamics, the hazard areas and the hazard levels of emergencies may vary from time to time. For example, the fire area and the hazard level of fire emergency events may increase as time goes by or decrease due to human intervention. Then during the navigation, the hazard potential of each node will not be stable for a rapid and safe navigation, which asks for estimating hazard speed and hazard level changes.

To estimate the speed of hazard, we have to find out the spread distance and the corresponding time. However, it is quite challenging to obtain the distance and time *distributedly* in a WSN-assistant navigation algorithm. Estimating the distance may need pre-knowledge of sensors location information as well as two or more sensors exchanging their readings, which may incur excessive communication costs, while obtaining the time may require relatively accurate time synchronization, which may rely on special hardware or time synchronization algorithms. These requirements are not suitable for resource-constrained WSNs and greatly hinder the designed algorithms from being distributed and lightweight. Thus, theoretically modeling the hazard speed in WSN-assistant navigation itself is still an open problem, and asks for thorough and intensive research [9], [12]. Therefore, existing navigation approaches mainly focus on the design of a navigation protocol, and deal with hazard

spread by incorporating a supplementary module in the manner of rebuilding the navigation architecture.

Unlike existing schemes, SEND takes the hazard level into account, and thus we have to consider both hazard speed and hazard level for avoid frequent updating the hazard potential field. We notice that the constructed hazard potential field reflects more global properties of the underlying hazard level distribution (i.e., nodes more closer to the hazard have higher hazard potential values, see Fig. 2), and thus SEND is more robust, to a certain extent, to hazard spread, since the navigation path provide the least hazard (proved by Theorem 2). Moreover, in our scenario, we assume hazard speed is less than peoples moving speed (otherwise, it may be impossible for a navigation algorithm to guide people near the hazard out of danger, e.g., in a terrorist bombing incident). Thus, SEND is able to complete the hazard potential field construction process before hazard spreads from one node to another. For instance, in the WSN deployed in a 3D building with 49 nodes in Fig. 7, the average distance between two nodes is around 30 meters. Assuming a 4 meter per second hazard speed, the hazard needs over 7 seconds spreading from one node to another, while SEND only consumes less than 4 seconds on average in our experiments. Therefore, we do not highlight hazard speed much, but only set a convergence threshold to avoid frequent updating the hazard potential (the implementation is detailed in Section 5), which is competent for a fast and safe navigation.

4.2 Reacting to Local Failures

In sensor networks, there may be temporary or permanent local node/link failures due to battery outage or environmental changes [3], [6]. This kind of local failures has some impacts on SEND, if a relatively large portion of sensor nodes are dead, and the network is no longer connected. Since one prerequisite of SEND is that the network should be connected, in such a case, sensor re-deployment has to be conducted such that the network can be connected.

However, as long as the network is connected, the impacts on SEND are limited. On one hand, the potential field can still be constructed, if the hazard potential $F(v)$ at the position of $v \in V_d \cup V_e$ is still constant. Even if $v \in V_d$ or $v \in V_e$ is destroyed, a simple scheme can be used to make up for it. To be more concrete, suppose node v senses the hazard, it then sets its hazard potential to be 1, and notifies its neighbors that it is in V_d . When v is destroyed, its neighbors set their immediate hazard potential to be constant. In this way, the iterative process of hazard potential field construction process is guaranteed to converge, and the potential field can thus be constructed.

On the other hand, the next hop selection during the navigation can still proceed, as current node always chooses the neighbor with the smallest hazardous potential among its neighbors as its next hop. It is noted that in our scenario the average node degree is above 5 (see Fig. 10), which means even one or two neighbor nodes are destroyed, there are still at least one neighbor available for the next hop node. In extreme situations, the current node faces the so-called local minima. In this case, a local random walk can be performed, as done in [27], [28], [29], to reach a nearby non-local minima node, so that the navigation can proceed without being suspended.

4.3 Impact of User Number and User Distribution

One may concern that when only a small number of users are trapped, the best way is to guide them to the nearest exit, to achieve a small detour. To enable such mechanism, however, two issues have to be addressed. First, to identify the nearest exit, we have to obtain the distance information. With mere connectivity information, the hop count distance in discrete WSNs may be used to approximate the distance, as done in most connectivity-based algorithms [27], [30], [31], [32]. On this basis, during the initialization phase of the network, each exit has to initiate a network wide flooding, so that each node in the network knows how far away it is from each exit. Second, to identify the number of users in a specific area (e.g., within one's five hop-count neighborhood), the users have to communicate to nearby nodes for several rounds, so that seeking for the nearest exit can be start up, which may need extra message cost.

Also, in our design, it would be more efficient for SEND in scenarios where users are relatively uniformly distributed in the field, e.g., in forest parks, amusement parks, campus laboratory buildings, etc. And SEND may not work that effectively in scenarios where a large group of users gather in a specific location, e.g., in concert halls or cinemas, as they may be guided to the same exit, thereby resulting in congestions. However, it is quite challenging to take user distribution into account in a fully distributed manner, as this may need global information, which is usually done by a central controller. What is more, it also needs extra message cost to obtain user distribution information.

As far as we know, the recently presented CANS algorithm [27] (a congestion-adaptive and small stretch emergency navigation algorithm with WSNs) can be combined with SEND, so as to enable situation-aware, mild congestion as well as small detour, at the same time. Interested readers may explore the possibility in the future.

5 IMPLEMENTATION

In Section 3, we have elaborated on our algorithm description and shown by theorems that the proposed algorithm guarantees successful navigation and generates optimal paths in terms of safety. In this section, we present the implementation of our algorithm in a real sensor network testbed, where every sensor node maintains a short list of variables, which record the status of this node, as shown in Table 2. The implementation process mainly consists of three steps: initialization, hazard potential field establishment and path construction.

In the initialization phase, all sensors keep sensing the environment and record the sensing data in *Reading* periodically. Based on the sensing data, each sensor node determines which role it plays in the network. Specifically, the sensor node sets its *Role* = 1, representing hazardous, when the sensing reading of a sensor node exceeds *Threshold*. Sensors, detected emergencies, set their *Potential* range from 0 to 1 according to their readings. The *Potential* of hazardous sensors is directly proportional to their sensed hazardous readings. Sensors with sensing readings at normal level (i.e., below *Threshold*) set their *Role* = 0, which represents no emergency happens. For sensors at exits, they set *Role* = -1, representing the destinations for emergency navigation,

TABLE 2
Sensor Data List

Byte #	Name	Description
0	<i>ID</i>	the unique ID of a sensor
1-2	<i>Reading</i>	the raw sensor reading
3	<i>Threshold</i>	determining whether a sensor is hazardous
4-7	<i>Criteria</i>	the criteria determining the hazard level
8	<i>Role</i>	the role of a sensor in a network
9-10	<i>Potential</i>	the hazardous potential
11	<i>Parent</i>	the ID of the parent sensor
12-18	<i>Neighbors</i>	the neighbors' IDs of a sensor
19-22	<i>Series</i>	the preceding <i>Potential</i>
23	<i>Converge</i>	the convergence threshold
24-40	<i>NPotential</i>	the <i>Potential</i> of neighbors

and their *Potential* range from -1 to 0 according to their evacuation capabilities. The higher evacuation capability of the exit, the smaller *Potential* value will be.

Next, we establish the hazard potential field. As discussed in Section 3, for the sensors in hazardous areas and at locations of safe exits, they set their *Potential* varies along with the environmental condition and diffuse their *Potential* to the network by conducting Eq. (8). The sensors playing hazardous roles and safe roles fix their *Potential* respectively and keep sending messages containing *ID* and *Potential* to their neighbors. For normal sensors, they keep examining their neighbors' *Potential* and conduct the accelerated hazard potential field establishing method as described in Section 3. By such means, the hazard potential field evolves and finally converges to a stable state, where *Potential* satisfies Eq. (8) at every normal sensor as shown in Fig. 2.

Based on the established hazard potential field, we can easily find out emergency navigation paths using the greedy method as discussed in Section 3. In particular, each sensor v selects among its neighbors (v . *Neighbors*) the one with the smallest *Potential* and sets its *ID* to be v . *Parent*. As proved in Section 3, the proposed evacuation navigation approach guarantees the successful navigation of the trapped users and is optimal in terms of safety.

Note that constrained by the computational accuracy of the microprocessor, the established hazard potential field may come across a plateau region where all neighbors of sensor v have the same hazard potential. This plateau region may lead to the failure of path planning due to the lack of accuracy of the computation in sensor node and the irregularity of the sensor distribution. In this case, the current node will search its local neighborhood through either a random walk or a local flooding can be performed to reach a nearby non-stationary node, so that the path planning can proceed without being suspended [28], [29].

At last, to react to emergency dynamics, we set a convergence threshold *Converge* to decide whether the iteration process of the hazard potential field construction should be continued or not. Note that the threshold *Converge* can be preloaded on all sensor nodes. When a sensor node v detects that Eq. (8) is violated, it conducts the computation in Eq. (9). Then, by comparing the newly computed *Potential* and its current s . *Potential*, only when $|s$. *Potential* ^{$k+1$} $- s$. *Potential* ^{k} $| > s$. *Converge*, the sensor node s replaces its current s . *Potential* by the newly

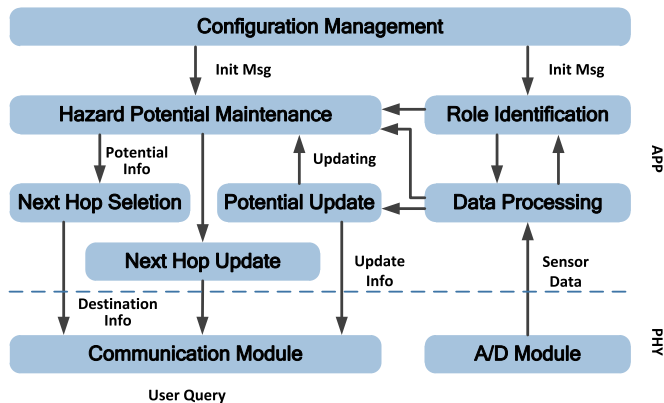


Fig. 4. Architecture of the experiment testbed.

computed *Potential*. After updating *Potential*, the sensor sends a message containing the updated hazard potential value to its neighbors, so that the neighbor nodes can update their *NeighborPotential*. Note that in our real testbed experiments, the time for the hazard potential field establishment is around 4 and 7 seconds in 2D and 3D, respectively, which provides a reference for choosing an appropriate value of *Converge* in a specific application.

6 EXPERIMENTAL RESULTS

This section describes the experimental results of the proposed algorithm on a testbed with TI CC2530 chips. The chip has 256 KB In-System-Programmable Flash and 8 KB SRAM. The operating system of the sensors is *Tiny OS*. The architecture of the testbed is shown in Fig. 4. The information of the sensor, including sensor ID, convergence threshold, role detection threshold, safe exit information, etc, is in the charge of the configuration management component. The communication module receives queries from trapped users and sends the path information back to them. It also takes charge of notifying its neighbor sensors the hazard potential status.

6.1 2D Experiments

We first implement the proposed algorithm on a testbed of 45 sensor nodes and deploy them on a roof of a building as a miniature prototype. The 45 sensors are deployed into grids with 1 meter space between a pair of nodes, as shown in Fig. 5. We conduct four experiments to examine our algorithm in the 2D field. The settings of the emergencies and exits in the four experiments correspond to the settings of the areas in Figs. 1 and 2, respectively.

The objective of the first two experiments is to test the impact of different hazard levels of emergencies on our algorithm. Initially, in the first experiment, two sensors are emergencies with *Potential* = 1 and one sensor is an exit with *Potential* = -1 . In the second one, we change the settings of the two sensors of emergencies with the top-left node's *Potential* = 1 and the bottom-right node's *Potential* = 0.5. The rest of the sensor nodes have *Potential* = 0, which means they are unaware of surrounding situations. When these settings are done, the network conducts the iteration process as in Eq. (9) to form the hazard potential field. Once the iteration process stops, each sensor node sets its neighbor node with the minimum *Potential* among all neighbors as its *Parent*. Eventually, each node

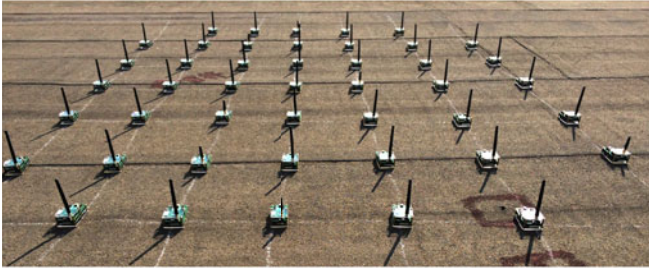


Fig. 5. Experiment testbed with sensors deployed in 2D space.



Fig. 7. Experiment field of a 3D building (top view).

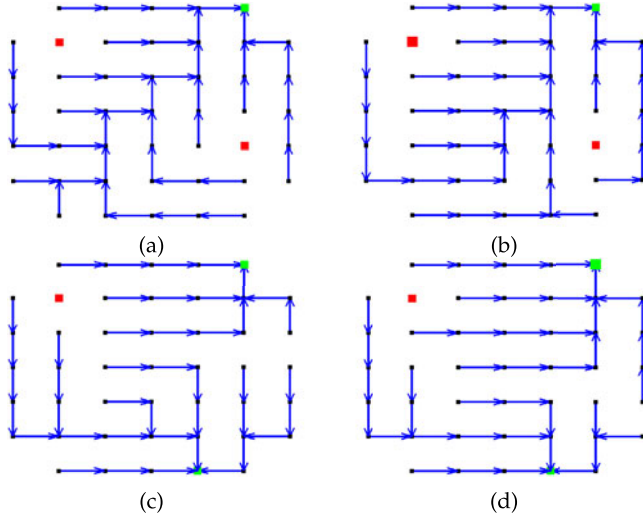


Fig. 6. Testbed experiments in the 2D scenarios of Fig. 1. (a) Navigation paths when equal hazard levels of emergencies exist. (b) Navigation paths when the hazard level is higher at the top-left red point and lower at the bottom-right one. (c) Navigation paths when the two exits marked in green have equal evacuation capabilities. (d) Navigation paths when the top-right exit has higher evacuation capability than the bottom-right one.

has a *Parent* node except for the nodes with hazardous readings and the nodes at positions of exits. As a result, nodes in the sensor network form path graphs shown in Figs. 6a and 6b. According to the path graphs, users in the sensing field could follow these paths to the safe exit. We can see from Figs. 6a and 6b, the navigation paths tend to keep equal distances to the two nodes with equal hazard levels but closer to the node with lower hazard level.

The objective of the last two experiments is to test the impact of different evacuation capabilities of exits on our algorithm. We set one sensor to be emergency with $Potential = 1$ and two sensors to be exit nodes with $Potential = -1$ in the third experiment. In the fourth experiment, we set $Potential = -1$ of the top-right exit node and $Potential = -0.5$ of the bottom-right exit node. The rest of the sensor nodes are set $Potential = 0$. Then, we conduct the same process in the former two experiments and obtain the path graphs shown in Figs. 6c and 6d. It is observed that the navigation paths tend to be attracted by the exit with higher evacuation capability. As can be seen in the four experiments, our algorithm can provide users emergency navigation service that has the capability to adapt the navigation paths to different situations.

6.2 3D Experiments

To validate the correctness of our algorithm in 3D scenarios, we implement a testbed in a 3D building as

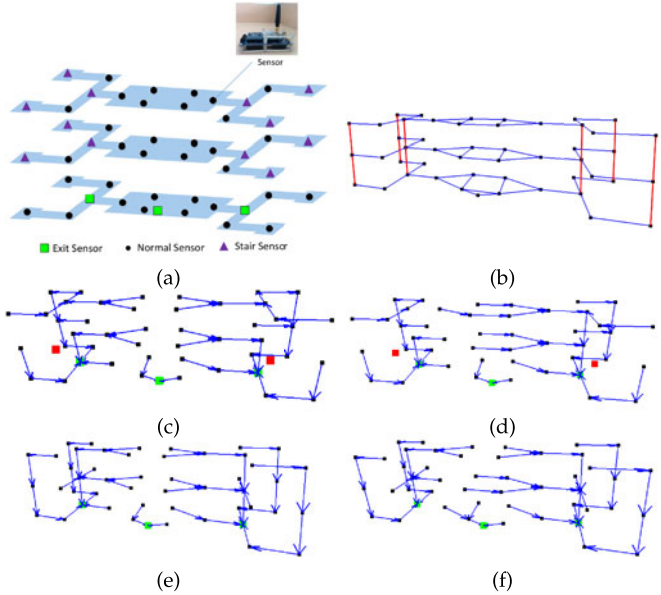


Fig. 8. Experimental results in a 3D building shown in Fig. 7. (a) The deployment of the sensor network. (b) The connectivity of the 3D sensor network; red lines indicate the edge between two stair sensors. (c) Navigation paths when the three exits have equal evacuation capabilities. (d) Navigation paths when there exist two sensors sensed dangers (the sensor in the west sense a higher hazard level). (e) Navigation paths when the three exit sensors have equal potentials. (f) Navigation paths when east and middle exits have higher evacuation capabilities than the west one.

shown in Fig. 7. The deployment and the connectivity of the sensors are shown in Figs. 8a and 8b. The building has three exits as shown by green squares in Fig. 8a. Similar with the 2D experiments, we conduct two groups of experiments.

For the first group of experiments, we test the impact of different hazard levels of emergencies on our algorithm. In the first experiment, two sensors are set as emergencies with $Potential = 1$, and the sensors at positions of exits are set the same evacuation capabilities with $Potential = -1$. In the second one, we change the hazard level of the right emergency to be less hazardous with $Potential = 0.5$. After conducting our algorithm, the path graphs established with different settings are shown in Figs. 8c and 8d. It is shown that the established navigation paths are inclined to avoid the sensors with higher hazard level.

The objective of the second group of experiments in 3D scenarios is to test the impact of evacuation capabilities of exits on our algorithm. In the third experiment, we set three exits the same evacuation capabilities with $Potential = -1$ and no sensors sensed emergencies. In the fourth one, we

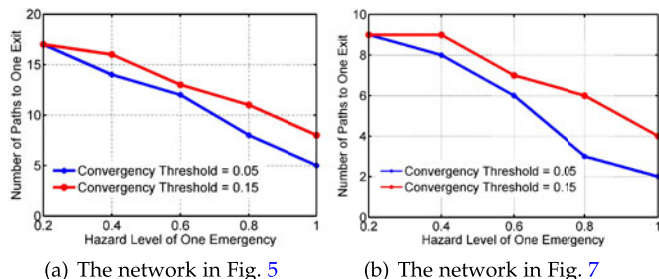


Fig. 9. Impacts of emergency dynamics and the convergence threshold.

set the three exit sensors different evacuation capabilities: the exit sensor at the western part of the building has the least evacuation capability with $Potential = -0.5$, and the other two have equal evacuation capabilities with $Potential = -1$. After conducting our algorithm, the established path graphs are shown in Figs. 8e and 8f. We can see from the results that exits with higher evacuation capabilities cover a larger area of sensing field than exits with lower evacuation capability. As can be seen in the four 3D experiments, our algorithm can also provide the correct solution in 3D scenarios.

6.3 Impact of Emergency Dynamics

To test the performance of SEND in the presence of emergency dynamics, we conduct further experiments in the 2D network in Fig. 5 and 3D network in Fig. 7. In the 2D network, we set two emergencies as in Fig. 5b and two exits as in Fig. 5d, where the hazard level of the top-left (resp. bottom-right) emergency is variable (resp. 0.5), and the capability of the top-right (resp. bottom-left) exit is -1 (resp. -0.5). We then randomly choose 20 nodes as the trapped users, and count their generated paths to the top-right exit. Intuitively, when the hazard level of the top-left emergency increases, the number of paths to the top-right exit will decrease. Fig. 9a demonstrates the experiment results when the convergence threshold is set 0.05 and 0.15, which is in accordance with the intuition. We can also find that, when the convergence threshold is small, the reacting speed to emergency dynamics is faster, as it is more sensitive to the change of hazard level of the emergency.

Similarly, in the 3D network, we set two emergencies and three exits as in Fig. 7c, where the hazard level of the left (resp. right) emergency is variable (resp. 0.5), and the capability of the left (resp. middle, right) exit is -1 (resp. -1 ,

-0.5). We also randomly choose 20 nodes as the trapped users, change the hazard level of the left hazard and count their generated paths to the top-right exit. Similar results are obtained, as shown in Fig. 9b.

7 SIMULATION RESULTS

The realistic testbed experiments testify the feasibility of our algorithm for small scale networks. In this section, we conduct extensive simulations by a simulator we developed using C++ in both 2D and 3D scenarios, to test the performance of our algorithm when the network size scales up. To construct the network topology, a set of nodes are randomly distributed on a 2D (e.g., Fig. 10) or 3D (e.g., Fig. 12) space. Once the nodes are placed, an appropriate maximum transmission range is identified to ensure that the network is connected. The constructed network topologies have an average node degree between 5 to 9.

We first test the impact of dynamic emergencies and exits by tuning the hazard levels of emergencies and the capabilities of exits. We then evaluate the hazard and the length of the selected paths by changing the network size. Finally, we test the performance of the proposed accelerated algorithm. The results show that our algorithm surpasses the road map navigation algorithm [10], [15] in terms of 31 percent reduction of the average path hazard and 17 percent reduction of the average path length.

7.1 The Impact of Emergencies and Exits

We emphasize that the ability to deal with different exit's capabilities and different hazard levels is the core advantage of our method. To test the impact of variant exit's capabilities and heterogeneous emergency events, we conduct simulations on the networks in Fig. 10 with various settings of obstacles, exits, emergencies. As shown in Fig. 10, the top-right and the bottom-left green triangles are exit nodes, marked as Exit 1 and Exit 2; the top-left and the bottom-right red squares are emergency nodes, marked as Hazard 1 and Hazard 2.

We first evaluate the impact of varying capabilities of the exits by randomly selecting 2,000 nodes (500 nodes in each network). We conduct the emergency navigation process by three approaches, i.e., our algorithm (SEND), greedy approach (GRD), and road map navigation approach [10]. Let us define the escape probability of one exit as the ratio of the path number of the exit to that of all exits. Then the

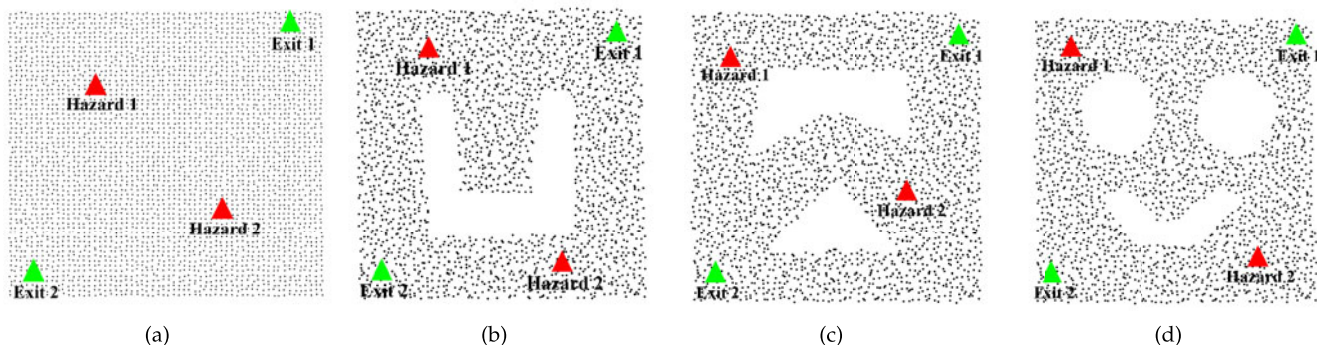


Fig. 10. Simulation networks. (a) A square network with 3,600 nodes; avg deg is 8.95. (b) A cup-shaped network with 2,901 nodes; avg deg is 7.88. (c) A wedge-shaped network with 2,113 nodes; avg deg is 6.91. (d) A smile-shaped network with 1,257 nodes; avg deg is 6.53.

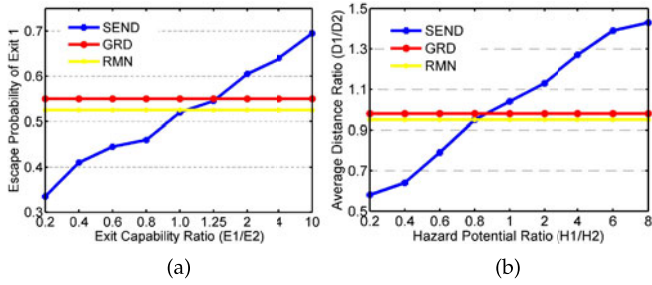


Fig. 11. Impacts of exits' capabilities and hazard levels of emergencies.

result in Fig. 11a shows that, for SEND the escape probability of Exit 1 increases as the exit capability ratio between Exit 1 and Exit 2 (Exit 1.Potential/Exit 2.Potential) increases. For GRD and RMN, the escape probability of Exit 1 is independent to the exit capability variation.

Second, we evaluate the impact of different hazard levels of emergencies by varying the hazard potential ratio between Hazard 1 and Hazard 2. It can be seen from Fig. 11b that, SEND has the ability to adjust the selected paths to keep further away from the emergency with higher hazard potential while the other two methods fail to take reaction to this kind of emergencies changes.

To intuitively demonstrate the effectiveness of our proposed approach in 3D sensor networks, we consider a sensor network deployed in a 3D genus-4 cube space, as shown in Fig. 12. In order to show the impact of the heterogeneous emergency events more clearly, we first test our algorithm with two hazardous regions and only one exit region. Figs. 12a and 12b depict the navigation results with different hazard levels. In Fig. 12a, the bottom-right area has higher hazard potential (1) than the top-left area (0.5) and in Fig. 12b, the bottom-right area has lower hazard potential (0.5) than the top-left area (1). The results show that the selected path is farther away from the area with higher hazard potential. To test the impact of multiple exits with different capabilities, we set two exits in the network as shown in Figs. 12c and 12d. We first set $Potential = -1$ of the middle-right area and $Potential = -0.5$ of the top middle area. In the other experiment, we exchange the settings of the two exit areas. The results show that, the exit area with higher evacuation capability is more attractive to the trapped users.

7.2 Hazard and Length of Selected Paths

We evaluate the hazard of the paths selected by our method and compare the results with RMN and the global exhaustive search scheme (OPT for short), which is optimal but impractical due to its inefficiency (note that here OPT is regarded as the ground truth). We select a number of paths under different network sizes and topologies in networks shown in Fig. 10, where the potentials of Exit 1, Exit 2, Hazard 1, and Hazard 2 are set -1 , -0.5 , 1 , and 0.5 , respectively. In these networks, we randomly select n paths (n equals half of the number of sensors in the network) and record the path hazard of each path $\Phi(p_i)$.

The average path hazard is defined as $\sum_n \Phi(p_i)/n$. Smaller average path hazard indicates higher safety of the selected path. It can be seen from Fig. 13 that OPT performs the best, while our approach performs as well as the optimal method, and outperforms RMN significantly. As discussed

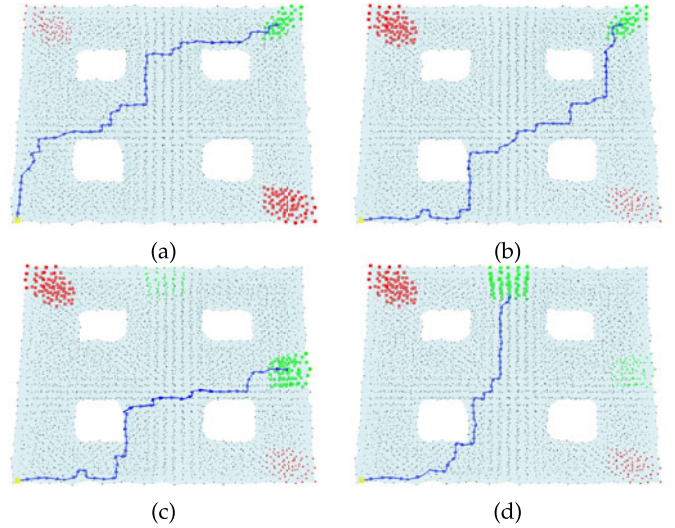


Fig. 12. Simulation results on a large-scale 3D high genus network with 4,085 nodes; average degree of 5.3. Nodes marked in red/green are hazards/safe exits; the trapped user is marked in yellow. (a), (b) The generated navigation path, which tends to avoid the sensor nodes with higher hazard potentials. (c), (d) The generated navigation path, which tends to be attracted by the exits with higher evacuation capabilities.

in Section 5, due to the limitation of computation accuracy and the irregularity of sensor distribution, we may conduct local random walk in a very small area to avoid the plateau phenomenon. As a result, the paths selected by our algorithm have a slightly higher average path hazard in comparison with OPT.

After the evaluation of the path safety, we next turn to path efficiency by comparing the average length of the selected paths. Similar with the safety evaluation, we randomly select n paths, and record the path length of each path L_i . The average path length is defined as $\sum_n L_i/n$. The smaller the average path length, the higher efficiency of the emergency navigation approach will be. As shown in Fig. 14, the average path length of our method is slightly higher than OPT and much better than RMN. This is because RMN has to search the path with the largest distance to hazardous regions and thus leads to an unnecessary long navigation path.

Note that we also evaluate the performance of SEND when there are three or four hazards. The results are with similar trend; the difference is that a slightly higher average path length is obtained, which is largely due to the detour around the hazard induced by more hazards.

7.3 The Convergence Speed of SEND

To evaluate the performance of our accelerated hazard potential establishing scheme, we conduct a simulation on the four networks in Fig. 10. In our simulations, we consider an interference-free link between a pair of nodes, as done in most connectivity based algorithms [30], [32], [33], [34]. Thus we use the iteration times as the metric.

We count the iteration times of all the 9,871 sensor nodes, and report the statistic results in Figs. 15 and 16. As shown in Fig. 15, the proposed accelerated iteration method has more than 2,600 sensors involved in the iteration times less than 20, and all the sensors are involved in the iteration times less than 60. Therefore, the accelerated method is

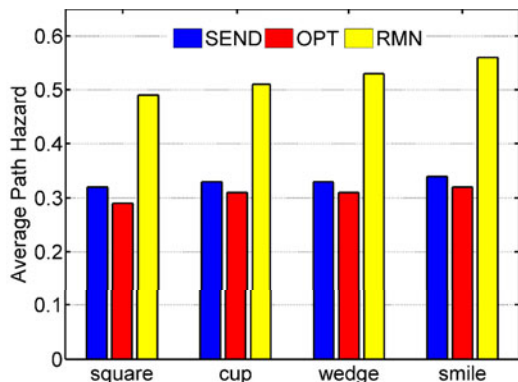


Fig. 13. Performance comparisons of the average hazard of the selected paths.

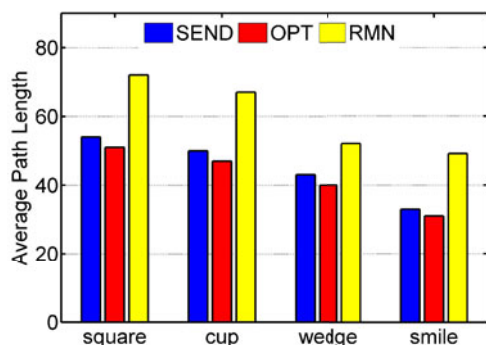


Fig. 14. Performance comparisons of the average length of the generated paths.

much faster than the normal method. We then randomly select one sensor and depict the relation between the iteration times and the hazard potential under different iteration methods. The result in Fig. 16 shows that our iteration scheme terminates about 37 rounds of iterations, which significantly boosts the convergence speed. Therefore, it can save the precious time for emergency navigation.

8 RELATED WORK

Navigation has been a crucial issue in such fields as robotics [35] and computational geometry [36] for a long time. Generating navigation paths with the assistance of WSNs, faces non-trivial challenges that are yet to be considered. The process is preferred to be conducted in a distributed manner, which is often over a self-organized network consisting of a huge number of sensor nodes. The traditional centralized path planning approach [37], [38], [39] is no longer viable, since the hop-by-hop communication over the shared wireless channel makes the data collection over multiple-hop routes to the sink node an extreme time-consuming task.

As such, the authors in [13] first proposed a distributed algorithm that finds the minimum exposure path. They adopted the artificial potential, which is derived from the hop counts between nodes, as the metric to compute the optimal navigation paths. The exit generates an attractive potential, pulling sensor nodes to it. At the same time, each emergency spot generates a repulsive potential, pushing sensor nodes away from it. Each node calculates its potential value, and the navigation path with the least

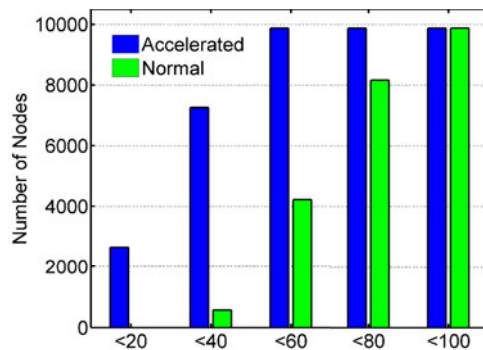


Fig. 15. Comparisons of the accelerated and non-accelerated hazard potential field establishing method; horizontal axis represents the iteration times.

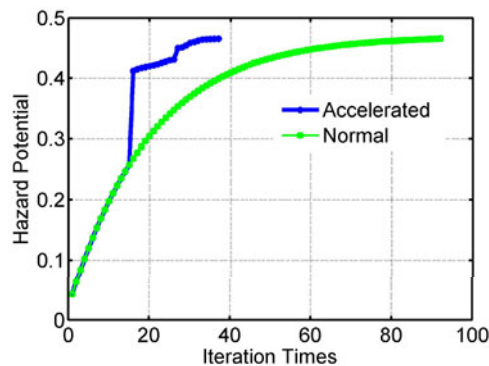


Fig. 16. The performance of the accelerated and non-accelerated hazard potential field establishing method for a randomly selected node.

total potential value is computed backward from the exit. One major concern of this approach is that it largely relies on exhaustive search and many rounds of flooding over the entire network to compute the navigation path with the least total potential value, thus it does not scales well.

To alleviate the high communication overhead for initializing paths caused by frequent flooding in [13], [14] proposed to abstract the field by the skeleton graph and accordingly find navigation routes over the skeleton graph. A skeleton graph is a sparse subset of the original network. Sharing information across the skeleton graph of a network saves the communication overhead of navigation. It requires the location information of each node. In most practical scenarios, location information is hard to obtain for a sensor network due to expensive cost of GPS and inaccurate in some condition such as indoor situation.

To this end, the authors in [10], [15] proposed a location-free protocol to navigate internal users along the medial-axis of the sensing field to a safe exit. The medial-axis can be efficiently and dynamically updated with the change of the emergencies. This method, however, is more likely to lead the users to emerging dangers for it guarantees the optimal safety on the medial axis, which may cause users moving back and forth and missing the precious chance to get to an exit. This kind of moving back and forth is called oscillation.

Taking oscillation into account, the authors in [9], [12] proposed OPEN, an oscillation-free navigation approach, which minimizes the probability of oscillation and guarantees

the success rate of emergency navigation. OPEN efficiently predicts the emergency dynamics in the navigation process and makes reliable decisions to guide users to the exit. Undesirably, it needs periodic flooding in the entire network, which is of high cost and does not scale well.

All of the existing studies do not take the impact of different hazard levels of emergencies and different capabilities of exits into account. They mainly treat emergencies equally and lead internal users to a nearby exit without considering the exit's evacuation capabilities. In addition, most if not all existing methods are designed for 2D settings, and thus cannot be directly applied to 3D scenarios.

9 CONCLUSION

This paper conducts the first work on situation-aware emergency navigation by considering a more general and practical problem, where emergencies of different hazard levels and exits with different evacuation capabilities may coexist. We first model the situation-aware emergency navigation problem and formally define the safety of a navigation path. We then propose a fully distributed algorithm to provide users the safest navigation paths, as well as an accelerated version that can significantly boost up the speed of the navigation. Both experiments and extensive simulations in 2D and 3D scenarios validate the effectiveness of SEND. We are currently devoting to conducting a small-scale system prototype under more complex scenarios. In the future, we would like to explore modeling the hazard speed in the context of emergency navigation. We also plan to cooperate with the local Fire Department to test our prototype, e.g., in the fire-fighting exercises, to provide more evidences on the real effects on user safety in real scenarios.

ACKNOWLEDGMENTS

This work was supported in part by the National Natural Science Foundation of China under Grants 61572219, 61502192, 61271226, 61272410, 61202460, and 61471408; by the National High Technology Research and Development Program ("863" Program) of China under Grants 2014AA01A701 and 2015AA011303; by the National Natural Science Foundation of Hubei Province under Grant 2014CFA040; by the China Postdoctoral Science Foundation under Grants 2014M560608; by the Fundamental Research Funds for the Central Universities under Grants 2015QN073, 2016YXMS297 and 2016JCTD118; and by the Science and Technology Plan Projects of Wuhan City under Grant 2015010101010022. The corresponding author of this paper is Hongzhi Lin.

REFERENCES

- [1] X. Xu, X. Li, and M. Song, "Efficient aggregation scheduling in multihop wireless sensor networks with SINR constraints," *IEEE Trans. Mobile Comput.*, vol. 12, no. 12, pp. 2518–2528, Dec. 2013.
- [2] L. He, Z. Yang, J. Pan, L. Cai, J. Xu, and Y. Gu, "Evaluating service disciplines for on-demand mobile data collection in sensor networks," *IEEE Trans. Mobile Comput.*, vol. 13, no. 4, pp. 797–810, Apr. 2014.
- [3] S. Lin, et al., "Toward stable network performance in wireless sensor networks: A multilevel perspective," *ACM Trans. Sensor Netw.*, vol. 11, no. 3, pp. 42:1–42:26, 2015.
- [4] S. Bondorf and J. B. Schmitt, "Boosting sensor network calculus by thoroughly bounding cross-traffic," in *Proc. 34th IEEE Int. Conf. Comput. Commun.*, 2015, pp. 235–243.
- [5] Y. Liu, X. Mao, Y. He, K. Liu, W. Gong, and J. Wang, "CitySee: Not only a wireless sensor network," *IEEE Netw.*, vol. 27, no. 5, pp. 42–47, Sep./Oct. 2013.
- [6] Y. Liu, Y. He, M. Li, J. Wang, K. Liu, and X. Li, "Does wireless sensor network scale? a measurement study on GreenOrbs," *IEEE Trans. Parallel Distrib. Comput.*, vol. 24, no. 10, pp. 1983–1993, Oct. 2013.
- [7] M. Li, Z. Yang, and Y. Liu, "Sea depth measurement with restricted floating sensors," *ACM Trans. Embedded Comput. Syst.*, vol. 13, no. 1, pp. 1:1–1:21, 2013.
- [8] M. Z. A. Bhuiyan, G. Wang, J. Cao, and J. Wu, "Sensor placement with multiple objectives for structural health monitoring," *ACM Trans. Sensor Netw.*, vol. 10, no. 4, pp. 68:1–68:45, 2014.
- [9] L. Wang, Y. He, Y. Liu, W. Liu, J. Wang, and N. Jing, "It is not just a matter of time: Oscillation-free emergency navigation with sensor networks," in *Proc. IEEE 33rd Real-Time Syst. Symp.*, 2012, pp. 339–348.
- [10] J. Wang, Z. Li, M. Li, Y. Liu, and Z. Yang, "Sensor network navigation without locations," *IEEE Trans. Parallel Distrib. Syst.*, vol. 24, no. 7, pp. 1436–1446, Jul. 2013.
- [11] E. Xu, Z. Ding, and S. Dasgupta, "Target tracking and mobile sensor navigation in wireless sensor networks," *IEEE Trans. Mobile Comput.*, vol. 12, no. 1, pp. 177–186, Jan. 2013.
- [12] L. Wang, Y. He, W. Liu, N. Jing, J. Wang, and Y. Liu, "On oscillation-free emergency navigation via wireless sensor networks," *IEEE Trans. Mobile Comput.*, vol. 14, no. 10, pp. 2086–2100, Oct. 2015.
- [13] Q. Li, M. De Rosa, and D. Rus, "Distributed algorithms for guiding navigation across a sensor network," in *Proc. 9th Annu. Int. Conf. Mobile Comput. Netw.*, 2003, pp. 313–325.
- [14] C. Buragohain, D. Agrawal, and S. Suri, "Distributed navigation algorithms for sensor networks," in *Proc. 25th IEEE Int. Conf. Comput. Commun.*, 2006, pp. 1–10.
- [15] M. Li, Y. Liu, J. Wang, and Z. Yang, "Sensor network navigation without locations," in *Proc. 28th IEEE Int. Conf. Comput. Commun.*, 2009, pp. 2419–2427.
- [16] J. H. Sorensen, B. L. ShumPERT, and B. M. Vogt, "Planning for protective action decision making: Evacuate or shelter-in-place," *J. Hazardous Mater.*, vol. 109, no. 1, pp. 1–11, 2004.
- [17] A. Braun, B. E. Bodmann, and S. R. Musse, "Simulating virtual crowds in emergency situations," in *Proc. 12th ACM Symp. Virtual Reality Softw. Technol.*, 2005, pp. 244–252.
- [18] B. E. Saltzman, "Preparation and analysis of calibrated low concentrations of sixteen toxic gases," *Anal. Chem.*, vol. 33, no. 8, pp. 1100–1112, 1961.
- [19] D. A. Crowl and J. F. Louvar, *Chemical Process Safety: Fundamentals With Applications*. Upper Saddle River, NJ, USA: Pearson Education, 2001.
- [20] ACT Emergency Services Agency. [Online]. Available: <http://www.esa.act.gov.au/>. Accessed online: Nov. 17, 2015.
- [21] J. San-Miguel-Ayanz, J. D. Carlson, M. Alexander, et al., "Current methods to assess fire danger potential," *Wildland Fire Danger Estimation Mapping—Role Remote Sens. Data.*, Singapore: World Scientific Publishing, 2003, pp. 21–61.
- [22] A. D. PolyaniN and A. V. ManzhIrov, *Handbook of Mathematics for Engineers and Scientists*. Boca Raton, FL, USA: CRC Press, 2006.
- [23] B. N. Clark, C. J. Colbourn, and D. S. Johnson, "Unit disk graphs," *Discr. Math.*, vol. 86, no. 1, pp. 165–177, 1990.
- [24] C. Zhang, J. Luo, L. Xiang, F. Li, J. Lin, and Y. He, "Harmonic quorum systems: Data management in 2D/3D wireless sensor networks with holes," in *Proc. 9th Annu. IEEE Commun. Soc. Conf. Sensor Mesh Ad hoc Commun. Netw.*, 2012, pp. 1–9.
- [25] L. N. Trefethen and D. Bau III, *Numerical Linear Algebra*. Philadelphia, PA, USA: Siam, 1997.
- [26] S. C. Chapra and R. Canale, *Numerical Methods for Engineers*. New York, NY, USA: McGraw-Hill, 2005.
- [27] C. Wang, H. Lin, and H. Jiang, "CANS: Towards congestion-adaptive and small stretch emergency navigation with wireless sensor networks," *IEEE Trans. Mobile Comput.*, vol. 15, no. 5, pp. 1077–1089, May 2016.
- [28] P. Skraba, Q. Fang, A. Nguyen, and L. Guibas, "Sweeps over wireless sensor networks," in *Proc. 5th ACM/IEEE Int. Conf. Inf. Process. Sensor Netw.*, 2006, pp. 143–151.
- [29] H. Lin, M. Lu, N. Milosavljevic, J. Gao, and L. J. Guibas, "Composable information gradients in wireless sensor networks," in *Proc. 7th IEEE/ACM Int. Conf. Inf. Process. Sensor Netw.*, 2008, 121–132.
- [30] J. Gao, L. Guibas, J. Gao, and L. Guibas, "Geometric algorithms for sensor networks," *Philosoph. Trans. Roy. Soc. A: Math., Phys. Eng. Sci.*, vol. 370, no. 1958, pp. 27–51, 2012.

- [31] G. Tan, H. Jiang, J. Liu, and A.-M. Kermarrec, "Convex partitioning of large-scale sensor networks in complex fields: Algorithms and applications," *ACM Trans. Sensor Netw.*, vol. 10, no. 3, pp. 41:1–41:23, 2014.
- [32] F. Li, C. Zhang, J. Luo, S.-Q. Xin, and Y. He, "LBDP: Localized boundary detection and parametrization for 3-D sensor networks," *IEEE/ACM Trans. Netw.*, vol. 22, no. 2, pp. 567–579, Apr. 2014.
- [33] G. Tan, S. A. Jarvis, and A.-M. Kermarrec, "Connectivity-guaranteed and obstacle-adaptive deployment schemes for mobile sensor networks," *IEEE Trans. Mobile Comput.*, vol. 8, no. 6, pp. 836–848, Jun. 2009.
- [34] Y. Yang, M. Jin, Y. Zhao, and H. Wu, "Distributed information storage and retrieval in 3-d sensor networks with general topologies," *IEEE/ACM Trans. Netw.*, vol. 23, no. 4, pp. 1149–1162, Aug. 2015.
- [35] S. Bhattacharya, N. Atay, G. Alankus, C. Lu, O. B. Bayazit, and G.-C. Roman, "Roadmap query for sensor network assisted navigation in dynamic environments," in *Proc. 2nd IEEE Int. Conf. Distrib. Comput. Sensor Syst.*, 2006, pp. 17–36.
- [36] M. De Berg, O. Cheong, M. Van Kreveld, and M. Overmars, *Computational Geometry: Algorithms and Applications*, 3rd ed. Berlin, Germany: Springer, 2008.
- [37] G. E. Jan, K. Y. Chang, and I. Parberry, "Optimal path planning for mobile robot navigation," *IEEE/ASME Trans. Mechatronics*, vol. 13, no. 4, pp. 451–460, Aug. 2008.
- [38] S. Bhattacharya, M. Likhachev, and V. Kumar, "Topological constraints in search-based robot path planning," *Auton. Robots*, vol. 33, no. 3, pp. 273–290, 2012.
- [39] M. Kuderer, C. Sprunk, H. Kretzschmar, and W. Burgard, "Online generation of homotopically distinct navigation paths," in *Proc. 31st IEEE Int. Conf. Robot. Autom.*, 2014, pp. 6462–6467.



Chen Wang received the BS and PhD degrees from the Department of Automation, Wuhan University, China, in 2008 and 2013, respectively. He is currently a postdoctoral fellow at the Huazhong University of Science and Technology, China. His recent research interests include wireless networking and mobile computing. He is a member of the IEEE.



Hongzhi Lin received the BS, MS, and PhD degrees from the Huazhong University of Science and Technology, China, in 2000, 2003, and 2008, respectively. He is currently an assistant professor and faculty member at the Huazhong University of Science and Technology. His current research interests include wireless networking and digital signal processing.



Rui Zhang received the BS degree in computer application technology from Jiangnan Petroleum Institution, China, in 2000, and the MA and PhD degrees in computer science from the Huazhong University of Science and Technology, China, in 2003 and 2012, respectively. She is an associate professor in the School of Computer Science and Technology, Wuhan University of Technology, China. Her research interests include network analysis, mobile computing, and data mining.



Hongbo Jiang received the BS and MS degrees from the Huazhong University of Science and Technology, China, and the PhD degree from Case Western Reserve University in 2008. After that, he joined as a faculty member at the Huazhong University of Science and Technology, where he is currently a full professor and a dean in the Department of Communication Engineering. His research concerns computer networking, especially algorithms, and protocols for wireless and mobile networks. He serves as an associate

editor of the *IEEE Transactions on Mobile Computing*, the *ACM/Springer Wireless Networks*, *Wiley Security and Communication Networks*, and an associate technical editor of the *IEEE Communications Magazine*. He is a senior member of the IEEE.

▷ For more information on this or any other computing topic, please visit our Digital Library at www.computer.org/publications/dlib.